

MASS DETERMINATION WITH GRAVITATIONAL MICROLENSING

Shude Mao¹ and Bohdan Paczyński²

¹ Max-Planck-Institute für Astrophysik, Karl-Schwarzschild-Strasse 1, 85740 Garching,
Germany

E-mail: smao@mpa-garching.mpg.de

²Princeton University Observatory, Princeton, NJ 08544–1001, USA

E-mail: bp@astro.princeton.edu

Subject headings: dark matter - gravitational lensing

ABSTRACT

We present a simple toy model of the distribution of objects responsible for gravitational microlensing. We use Monte Carlo simulations to demonstrate how difficult it is to determine the parameters of the lens mass distribution on the basis of the observed distribution of event time scales. A robust determination requires ~ 100 events, or more, even if the geometry of lens distribution, and the lens kinematics are known.

1. Introduction

One of the main objectives of the searches for microlensing events (Paczynski 1996, and references therein) is to determine the mass function of the lensing objects. The determination of typical lens masses, or even their distribution function, were attempted by Alcock et al. (1993), Udalski et al. (1994), Zhao et al. (1995, 1996), Han & Gould (1996), and many others.

We know that some lenses must be ordinary stars, but some may be brown dwarfs, and perhaps also planetary mass objects, and even more exotic things like black holes. It is recognized that even if all lensing objects were of the same mass M , they would give rise to a broad range of time scales t_0 of the observed microlensing events. Although this is known to a relatively small number of people in the field this fact is not generally appreciated. Considering the broad interest in the nature of dark matter, and the relevance of microlensing searches to this problem, we feel it is justified to present a very simple model of the lens distribution and kinematics which allows some results to be obtained

analytically, and the rest can be calculated with one-dimensional numerical integrals. This model retains some of the most important generic characteristics: a very broad distribution of t_0 with power law tails towards very short and very long time scales for a delta function distribution of lens masses. Using Monte Carlo simulations we demonstrate how difficult it is to obtain accurate information about the mass function even within the framework of our simple model. In reality one is not sure what is the correct space distribution and kinematics of lensing masses, making the interpretation even more difficult.

The model is described in the next section. The results of the Monte Carlo simulations are presented in section 3, and the discussion of the results is given in the last section. The technical details of the model can be found in the appendix.

2. A Model

We consider a simple case that may approximate a real astrophysical system: the lenses, each of the same mass M , have their distances D_d distributed uniformly and randomly between the observer and a stationary source, which is at a distance D_s . The time scale of a microlensing event is given by

$$t_0 = \frac{R_E}{V_t}, \quad V_t \equiv V \sin i, \quad (1a)$$

where V is the relative spatial velocity between the lens and the observer, i is the angle between the velocity vector and the line of sight, and R_E is the Einstein ring radius:

$$R_E = (2R_g D)^{1/2}, \quad R_g = \frac{2GM}{c^2}, \quad D = \frac{(D_s - D_d)D_d}{D_s}. \quad (1b)$$

More technical details about our model are given in the appendix. In this section we present only the most essential information.

The lenses in our model have a three-dimensional Gaussian velocity distribution with a one-dimensional dispersion of σ_V . A characteristic time scale for a microlensing event is defined as

$$t_\sigma = \frac{1}{\sigma_V} \left(\frac{GM D_s}{c^2} \right)^{1/2} = 70 \text{ days} \left(\frac{100 \text{ km s}^{-1}}{\sigma_V} \right) \left(\frac{M}{1 M_\odot} \right)^{1/2} \left(\frac{D_s}{8 \text{ kpc}} \right)^{1/2}. \quad (2)$$

The probability distribution for event time scales has power law tails:

$$P_\delta(< t) = \frac{2^{11/2}}{3\pi^{3/2}} t^3, \quad \text{for } t \ll 1, \quad (3a)$$

$$P_\delta(> t) = \frac{2^{11/2}}{45\pi^{3/2}} \frac{1}{t^3}, \quad \text{for } t \gg 1, \quad (3b)$$

where

$$t \equiv t_0/t_\sigma, \quad (3c)$$

and the subscript δ indicates that all the lenses have the same, i.e., we have a δ mass function. The full probability distribution of event time scales can be calculated numerically and it can be approximated within 6% with a formula

$$p_\delta(\log t) d \log t \approx \frac{ct^3}{1 + 15t^6} \times 10^{-1.44(\log t + 0.293) \exp[-((\log t + 0.28)/0.304)^2]} d \log t, \quad (4)$$

where

$$c = \frac{2^{5.5}}{\pi^{1.5}} \ln 10 \approx 18.71,$$

The first two moments and the standard deviation of this distribution are

$$\langle \log t \rangle_\delta \equiv \int_0^\infty p_\delta(t) \log t dt = -0.242, \quad (5a)$$

$$\langle (\log t)^2 \rangle_\delta \equiv \int_0^\infty p_\delta(t) (\log t)^2 dt = 0.116. \quad (5b)$$

$$\sigma_\delta \equiv \left[\langle (\log t)^2 \rangle_\delta - (\langle \log t \rangle_\delta)^2 \right]^{1/2} = 0.240. \quad (5c)$$

Naturally, formula (4) applies only to our simple model of the lens distribution and kinematics. However, the presence of power law tails is common to almost all distributions ever proposed (e.g., those in Zhao et al. 1996) and can be understood intuitively. The very long events are produced by the lenses which move almost along the line of sight. For these events the time scale t is inversely proportional to $\sin i$, i.e., $t \propto i^{-1}$ (cf. eq. 1a). The number of these events, N , is proportional to the solid angle $(1 - \cos i)$ divided by t , i.e., $N \propto (1 - \cos i)/t \propto i^3 \propto t^{-3}$. On the other hand, the short events are produced by the lenses which are very close to either the source or the observer. For the latter case, $t \propto R_E \propto D_d^{1/2}$, and the number of these events is $N \propto R_E^2 D_d/t \propto t^3$. The same argument applies when the lenses are close to the source.

It is not likely that all the lenses have identical masses, and it is convenient to consider a power law mass distribution

$$p(M) d\left(\frac{M}{M_0}\right) = A \left(\frac{M}{M_0}\right)^\alpha d\left(\frac{M}{M_0}\right), \quad \text{for } M_{\min} \leq M \leq M_{\max}, \quad (6a)$$

where

$$M_0 = (M_{\min} M_{\max})^{1/2}, \quad (6b)$$

and we denote the logarithmic width of the mass function by

$$\beta \equiv \log (M_{\max}/M_{\min}). \quad (6c)$$

The exponent $\alpha = -1.5$ corresponds to an equal rate of microlensing events per decade of lens masses, while the case $\alpha = -2$ corresponds to an equal contribution to the optical depth per decade of lens masses. For $-2 < \alpha < -1.5$, the optical depth (total mass) is dominated by the massive objects, while the event rate is dominated by the low mass objects. For a given mass range the standard deviation of $\log t$ is the largest for $\alpha = -1.5$. For $\alpha \ll -1.5$ the mass spectrum is dominated by low mass objects, and the event time scales have a small effective range, with the majority of events caused by lenses with $M \approx M_{\min}$. In the opposite case, with $\alpha \gg -1.5$, the microlensing events are dominated by lenses with $M \approx M_{\max}$. Therefore for $\alpha > -1.5$, the standard deviation in $\log t$ approaches some asymptotic value when $M_{\min} \rightarrow 0$, and similarly for $\alpha < -1.5$ when $M_{\max} \rightarrow \infty$. After some algebra one may show that the variance in the observed distribution of event time scales can be expressed as

$$\sigma_{\log t}^2 = \sigma_{\delta}^2 + \frac{\beta^2}{48}, \quad \text{for } \alpha = -1.5, \quad (7)$$

and the asymptotic value is

$$\sigma_{\log t, \infty}^2 = \sigma_{\delta}^2 + [2 (\alpha + 1.5) \ln 10]^{-2}, \quad \text{for } \alpha \neq -1.5, \quad \beta \rightarrow \infty, \quad (8)$$

where $\sigma_{\delta} = 0.240$, as given by eq. (5c).

The probability distribution functions for the logarithm of event time scale for any lens mass function can be calculated by convolving the mass function with the probability distribution for a δ mass function as given in eq. (4). The probability distributions for $(\alpha, \beta) = (-1.5, 1), (-1.5, 2), (-2.5, 1), (-2.5, 2)$, are shown in Fig. 1. All time scales are in units of t_{σ} corresponding to $M = M_0 \equiv (M_{\min}M_{\max})^{1/2}$ (cf. eqs. 2 and 6). Also shown is the case for $\beta = 0$, i.e., with all the lenses having identical masses (cf. eq. 4). The shapes for mass functions with a narrow width ($\beta \lesssim 1$) are quite similar. This can be easily understood because the time scale of microlensing $t_0 \propto M^{1/2}$, therefore one decade of mass range translates to a factor of three in the time scale, hence the shapes of these distributions still resemble that for a δ mass function.

3. Monte Carlo Simulations

We present two types of Monte Carlo simulations. In both cases we adopt the model of lens distribution and kinematics as developed in the previous section. First, we consider

a perfect detection system, which can detect every event of any time scale, and a lens population with a moderately broad power law mass function. Next we consider very broad lens mass functions and a detection system which is like that of the MACHO and OGLE collaborations, i.e., it has a significant detection efficiency over a relatively narrow range of event time scales. In both cases we make a large number of the Monte Carlo simulations to determine the accuracy with which the lens mass function parameters can be estimated with a moderately large number of detected events: $n = 10$, $n = 100$, and $n = 1,000$.

We tried both the moment method and the maximum likelihood method to estimate the parameters α and β . Although the moment analysis is faster and in many cases its results agree with that from the maximum likelihood, it is less accurate and in some cases does not work at all. One of the reasons is very easy to understand. Imagine we have a random sample of microlensing events with variance smaller than $\sigma_\delta = 0.240$, as given by eq. (5c). Such cases are unavoidable in a finite sample drawn from a distribution with $\sigma > \sigma_\delta$. The moment analysis fails for these cases. This reminds us of a similar old problem: what to do with negative trigonometric parallaxes of distant stars, the negative numbers being due to the unavoidable measurement errors? For this reason, we only present the results from the maximum likelihood method with a prior of equal probability in α and β . However, general discussions are given using the more intuitive moment analysis.

3.1. Finite Mass Range, Perfect Detection System

We adopt a power law lens mass function described with two dimensionless parameters: the power law exponent α , and the range of masses $\beta \equiv \log (M_{\max}/M_{\min})$ (cf. eq. 6). In addition, we have two scaling parameters: A and $M_0 \equiv (M_{\min}M_{\max})^{1/2}$ (cf. eq. 6). Other things being equal the optical depth and the rate of microlensing events are proportional to A , while the average time scale of the events is proportional to $M_0^{1/2}$. Out of the four parameters, the scaling parameter A can be fixed by the observed event rate, after which we are still left with three parameters. We can simplify the problem further by identifying a mass scale in the problem. In most cases, we assume such a scale is provided by a fixed upper mass limit, say $M_{\max} = 1M_\odot$, but we also explore another possibility (see below).

We assume that the lens detection system is perfect, i.e., it is 100% efficient for all event time scales. A large number of Monte Carlo samples are generated with the *average* number of events $n = 100$ and $n = 1,000$. The actual number of events was chosen from a Poisson distribution, followed by a Monte Carlo selection of event time scales according to the model probability distributions, as shown in Fig. 1.

We selected two models with $(\alpha, \beta) = (-1.5, 1)$, $(-1.5, 2)$, each for two sample sizes: $n = 100$ and $n = 1000$. The 1σ and 2σ contours are shown in Fig. 2. It is clear that for the case of $(\alpha, \beta) = (-1.5, 1)$, the power law index α cannot be determined very well with 100 events, the case for $(\alpha, \beta) = (-1.5, 2)$, however, is improved. The large difference between $\beta = 1$ and $\beta = 2$ is because for $\beta = 1$, the shapes, and therefore the variances, of the duration distributions for different power law indices are similar (cf. Fig. 1). The main difference between the models is the average duration, i.e., the first moment of the duration distribution. However, such difference can be accommodated by slightly changing the lower mass limit. The power law index α is then mostly constrained by the more uncertain higher moments, and hence the weak limit.

The case with a broader mass function, $\beta = 2$, is better constrained than that for $\beta = 1$ with a sample of $n = 100$ microlensing events, but even this case is very poorly constrained when $n = 10$, as shown with the dotted contours in Fig. 2. Note that the total number of microlensing events detected so far towards the LMC is smaller than 10 (Bennett et al. 1996) and the spatial distribution and kinematics of the lenses are not known, making the case even more ill-constrained.

The contours shown in Fig. 2 are based the assumption that the upper mass limit is known. Such a fixed upper limit sets the mass scale in the maximum likelihood method and translates the observed average duration (i.e., the first moment of the duration distribution) into a constraint on the lower mass limit. In reality, we do not know the upper mass limit well. In fact, this upper limit should also be found from the maximum likelihood. However, it is too time consuming to conduct such a three dimensional study. Instead we adopt a different approach: for a given set of (α, β) , we fix the mass scale such that it gives identical first moment in the duration distribution as a generated Monte Carlo sample. This reduces the three-dimensional problem into a two dimensional one, and should be a reasonable approximation. As the first moment has been utilized to set the mass scale, the determination of α and β is then effectively based on the second and higher moments, and these are subject to larger random uncertainties. The likelihood contours shown in Fig. 2 confirms this for $\alpha = -1.5, \beta = 2$ with $n = 100$ (dashed lines). Just as expected, the limit is relaxed – the allowed parameter space is increased by a factor of ≈ 2 . This is a consequence of the determination made with the maximum likelihood (or any other) method effectively using the higher moments of the event distribution.

With the Monte Carlo samples, we can also estimate the optical depth of microlensing, τ , which is proportional to the number of events observed per unit time per unit number of stars. The error of the optical depth estimate is inversely proportional to the square root of the number of events, $n^{-1/2}$, with a coefficient somewhat larger

than unity, as the relatively few longest events are most important. This coefficient depends on the values of α and β . For example, the coefficients are 1.3, 1.5, 1.3, 1.6 for $(\alpha, \beta) = (-1.5, 1), (-1.5, 2), (-2, 1), (-2, 2)$, respectively. This is in good agreement with Han & Gould (1995). If we have 100 microlensing events, and if we can trust our model of the lens distribution and kinematics, then we can estimate the value of τ with an accuracy of $\approx 15\%$.

3.2. Very Broad Mass Range, Imperfect Detection System

Now we consider a very broad mass function with $\beta \gg 1$, so the time scales of microlensing events cover the range $\Delta \log t_0 \approx 0.5\beta$. We adopt the efficiency of event detectability similar to those published by the OGLE (Udalski et al. 1994) and MACHO (Alcock et al. 1995a) collaborations. We approximate the detection efficiency with a formula:

$$\epsilon = \begin{cases} 0.4 \exp[-(\log t)^2/0.72], & \text{if } \log t < 0 \\ 0.4 \exp[-(\log t)^2/0.18], & \text{if } \log t > 0 \end{cases} \quad (10)$$

where $t \equiv t_0/t_p$, and $t_p \approx 35$ days corresponds to events with durations that are at the peak of detection sensitivity. The detectability window as described by eq. (10) has a width of about one decade at half maximum. Using eq. (2) we may relate this time scale to a mass scale

$$M_p = 0.25M_\odot \left(\frac{\sigma_V}{100 \text{ km s}^{-1}} \right)^2 \left(\frac{8 \text{ kpc}}{D_s} \right). \quad (11)$$

Again we adopt a power law mass function as given by eq. (6). It is convenient to express the lower and upper mass limits in units of M_p with $\beta_{\min} \equiv \log (M_{\min}/M_p)$ and $\beta_{\max} \equiv \log (M_{\max}/M_p)$. The probability distributions of event time scales for very broad mass functions, with $\beta = 10$ and slopes $\alpha = -2, -1.5, -1$, are shown in Fig. 3. Also shown is the efficiency of event detection as described with eq. (10).

If the probability function of event time scales is much broader than the width of the detectability window as given by eq. (10) then most events cannot be detected. We shall consider two cases. First, a mass function extending very far towards low masses, i.e., with $\beta_{\min} \ll -1$, and the upper mass limit somewhat larger than M_p . Second, a mass function extending very far towards large masses, i.e., with $\beta_{\max} \gg 1$, and the lower mass limit somewhat smaller than M_p . We shall investigate the ability of the detection system to measure β_{\max} in the first case, and β_{\min} in the second case.

In all the simulations we adopt the average number of detected events to be either $n = 100$ or $n = 1,000$, the actual number being drawn from a Poisson distribution.

Assuming that $\beta_{\min} \ll -1$ we can search for the remaining two dimensionless parameters: α and β_{\max} using the maximum likelihood method, with A being fixed by the event rate. The results of model calculations are shown in the right panel of Fig. 4 for $(\alpha, \beta_{\max}) = (-1.5, 1)$, and $(-1.5, 2)$. With 100 events, α is well constrained in both cases. The parameter β_{\max} , however, becomes not so well-determined for $\beta_{\max} = 2$.

Assuming that $\beta_{\max} \gg 1$ we can search for the remaining two dimensionless parameters: α and β_{\min} using the maximum likelihood method. The results of model calculations are shown in the left panel of Fig. 4 for $(\alpha, \beta_{\min}) = (-1.5, -3), (-1.5, -2)$, and $(-1.5, -1)$. The parameter α is again well constrained for $n = 100$. In comparison, the parameter β_{\min} becomes ill-determined when it approaches -3 .

Note that the models with $\beta_{\min} = -3$ and $\beta_{\max} = 2$ have contours slightly shifted with respect to the true model values, as marked with crosses. If the distribution of event time scales is approaching the effective edge of the detectability window then some finite samples of events generate second (and other) moments which are incompatible with the model. For such cases a method using the moments simply fails. The maximum likelihood method can better handle such cases, but has some trouble as well for $n = 100$, as indicated by the small shifts of contours in Fig. 4. This can be remedied with a larger sample size such as $n = 1000$ (thick dashed lines) in both cases.

Given the determination of α and either β_{\min} or β_{\max} , as well as the ‘observed’ number of events ‘ n ’ we may estimate the parameter A in eq. (6). The error of the estimate can be written as

$$\sigma_A \approx a n^{-1/2}, \quad (12)$$

where σ_A is the standard deviation in the $A_{\text{sample}}/A_{\text{model}}$ ratio. The coefficient a depends somewhat on α and β , but is generally in the range between 1 and 1.6.

4. Discussion

The Monte Carlo simulations presented in this paper demonstrate that even if we have a full knowledge of the space distribution and kinematics of the lensing objects, or equivalently, if we know the relation between the lens mass and the distribution of event time scales (see eq. 4 for an example), it may still be difficult to obtain the parameters of the lens mass function. The problem is particularly serious when the width of the mass function is narrow ($\beta \lesssim 1$). In addition, if the mass function power law is quite different from -1.5 , then it will be difficult to probe the high mass end when $\alpha \ll -1.5$, and the low mass end when $\alpha \gg -1.5$ (cf. eq. 8).

Recently, Han & Gould (1996) obtained a rather tight limit on the mass function of the Galactic disk using about 50 microlensing events toward the Galactic bulge. In their analysis, the upper mass limit is fixed at $10M_{\odot}$ in a rather ad hoc manner. As we have shown in Fig. 2, such a fixed upper mass limit will make the determination of the other parameters appear more accurate. A more realistic approach is to estimate the upper mass limit using the maximum likelihood in order to avoid carrying our a priori assumption into a limit on the physical parameters. In general, if at least three separate parameters are to be estimated, for example M_0 , α , and β , then any method must effectively use the information contained in at least the first three moments. However, the higher the moment the more uncertain is its value as estimated from a relatively small sample of events. Therefore, the accuracy of the determination of any distribution parameter is lower in the 3-parameter determination than in a 2-parameter determination. Unfortunately, the smaller errors in a 2-parameter determination could be misleading, unless we have an independent and reliable information about the value of the third parameter.

In our second example, very broad mass functions are sampled through a realistic detectability window (cf. Fig. 4). The current published sensitivity windows allow one to probe about three to four decades of mass range and we find that the “amplitude” A and the local slope of the lens mass function α can be determined reasonably well with ~ 100 events. However, the estimate of the range of masses within the detectability window, β_{\min} or β_{\max} , may be very uncertain with as many as $n = 100$ events, as shown in Fig. 4.

If the mass function is broader than the detectability window then the total event rate or the total optical depth (or total mass) cannot be measured as the majority of events are outside the detectability window (Fig. 3), having either too short or too long t_0 . This points to the necessity of broadening the detectability window, a task easy to accomplish in the near future. Some first attempts have already been made by the EROS (Ansari et al. 1995) and MACHO collaborations (Bennett et al. 1996).

How can we be sure that we have reached the low and the high mass end of the lens distribution? In principle this is simple: we have to broaden the detectability window and we should detect so many events that the generic power law tails in the distribution (cf. eq. 3) become apparent. This may call for well over 100 events. Such a high number of events is within reach for the Galactic Bulge, where the rate appears to be very high (Udalski et al. 1994, Alcock et al. 1995b,c). The determinations of any parameters of the distribution of lens masses based on as few as 10 events are subject to very large uncertainties, as shown with the dotted contours in Fig. 2.

In reality we do not know what the geometry of the lens distribution is, and what is the lens kinematics. While looking towards the Galactic Bulge the majority of lenses may

be in the Bulge itself (Kiraga & Paczyński 1994, Udalski et al. 1994, Paczyński et al. 1994, Zhao et al. 1995, 1996), or they may be in the disk (Alcock et al. 1995b,c). While looking towards the LMC the majority of lenses may be in our galaxy (Alcock et al. 1995a) or in the LMC (Sahu 1994; Wu 1994). Depending on the location and kinematics the relation between the lens masses and the event time scale t_0 may be very different, and this leads to an additional major uncertainty on top of purely statistical uncertainty discussed in this paper. It seems rather difficult to disentangle all parameters one needs to describe the distribution and kinematics of the lenses *and* their mass function on the basis of the observed distribution of event time scale.

Fortunately, the future studies of the variation of the optical depth with the location in the sky will help to identify the lens location. If lensing of the Galactic Bulge stars is dominated by the Bulge lenses then the optical depth should vary rapidly with the galactic longitude (Kiraga & Paczyński 1994). If such a variation is not present this will indicate that the lenses are located mostly in the galactic disk. If lensing towards the LMC is dominated by the LMC lenses then the optical depth should increase strongly towards the LMC center (Sahu 1994). If the optical depth is uniform over the LMC then the lenses must be mostly in our galaxy. This is very simple in principle, but it will take hundreds of events to establish beyond reasonable doubt. Such a large number will be readily collected towards the Galactic Bulge, but it will take a very long time for the LMC as the rate in that direction is very low (Alcock et al. 1995a). Once the geometry of the lens distribution is established it will be possible to develop reliable models of their kinematics, and infer a reasonable statistical relation between the lens masses and the event time scales t_0 .

This project was supported by the NSF grant AST93-13620 and by the “Sonderforschungsbereich 375-95 für Astro-Teilchenphysik” der Deutschen Forschungsgemeinschaft. We are very grateful to Dr. Peter Schneider for a critical reading of the manuscript.

A. Appendix

We begin with the simplest lens model: all lensing objects have the same mass M , the same three-dimensional velocity V , and their velocity vector directions have a random isotropic distribution. The source located at the distance D_s is stationary, and the number density of lensing objects is uniform between the observer and the source.

If all the events had identical time scales, then the number of microlensing events expected in a time interval Δt would be given as

$$N = \frac{2}{\pi} n_s \tau \frac{\Delta t}{t_0}, \quad \text{for } t_0 = \text{const}, \quad (\text{A1})$$

where $2/\pi$ is the ratio of Einstein ring diameter to its area, in dimensionless units, n_s is the number of sources monitored, and τ is the optical depth of microlensing. In fact there is a broad distribution of event time scales as lenses have transverse velocities in the range of $0 \leq V_t \leq V$, and distances in the range $0 \leq D_d \leq D_s$. A straightforward but tedious algebra leads to the equation

$$N = \frac{3\pi}{16} n_s \tau \frac{\Delta t}{t_m} = N \int_0^\infty p_0(t_0) dt_0, \quad (\text{A2a})$$

where

$$t_m \equiv \left(\frac{R_E}{V} \right)_{D_d=0.5D_s} = \left(\frac{GMD_s}{c^2} \right)^{1/2} \frac{1}{V}, \quad (\text{A2b})$$

is the time scale for a microlensing event due to a lens located half way between the source and the observer, and moving with the transverse velocity V , and the probability distribution of event time scales is given by

$$p_0(t_0) dt_0 = p_T(T) dT \equiv \frac{1}{\pi^2 T^3} \left[-6T(1+T^2) + (3+2T^2+3T^4) \ln \left| \frac{1+T}{1-T} \right| \right] dT, \quad (\text{A3a})$$

where

$$T \equiv \frac{t_0}{t_m}, \quad 0 < t_0 < \infty. \quad (\text{A3b})$$

The probability distribution diverges logarithmically at $t_0 = t_m$, however, the integrated probability converges. Also note that the probability density distribution satisfies: $p_0(1/T) = T^2 p_0(T)$. Therefore, the probability that the event time scale is longer than $T (> 1)$ is equal to the probability that the time scale is shorter than T^{-1} .

The asymptotic behaviors of the integrated probability are given by

$$P_0(< T) = \frac{128}{45\pi^2} T^3, \quad \text{for } T \ll 1, \quad (\text{A4a})$$

$$P_0(> T) = \frac{128}{45\pi^2} \frac{1}{T^3}, \quad \text{for } T \gg 1. \quad (\text{A4b})$$

The power law tails are generic to almost all lens distributions ever proposed. Also note that only the first two moments of the distribution are finite: $\langle t_0 \rangle$ and $\langle t_0^2 \rangle$, while the third and higher moments diverge. Therefore, it is convenient to use a logarithmic probability distribution defined as

$$p_0(\log t_0) d \log t_0 = (\ln 10) t_0 p_0(t_0) d \log t_0, \quad (\text{A5})$$

as all moments of this distribution are finite.

Now we shall convolve the results obtained above with a three-dimensional Gaussian distribution adopted for the lens velocities:

$$p(V) dV = \left(\frac{2}{\pi}\right)^{1/2} \exp\left(-\frac{V^2}{2\sigma_V^2}\right) \frac{V^2}{\sigma_V^2} \frac{dV}{\sigma_V}, \quad (\text{A6})$$

where σ_V is the one-dimensional velocity dispersion, related to the three-dimensional velocity dispersion by $\sigma_V = V_{rms}/\sqrt{3}$. The total number of events expected from the lenses with such a distribution of velocities is given by

$$N_\delta = \left(\frac{9\pi}{32}\right)^{1/2} n_s \tau \frac{\Delta t}{t_\sigma}, \quad (\text{A7a})$$

where

$$t_\sigma = t_m(V = \sigma_V) = \frac{1}{\sigma_V} \left(\frac{GMD_s}{c^2}\right)^{1/2}. \quad (\text{A7b})$$

and the subscript δ indicates that all the lenses have identical masses, i.e., the mass function is a δ function.

After some algebra, the probability distribution of event time scales can be written as

$$p_\delta(t) = \frac{1}{2} \int_0^\infty \exp\left(-\frac{v^2}{2}\right) v^4 p_T(vt) dv, \quad t = \frac{t_0}{t_\sigma}, \quad v = \frac{V}{\sigma_V}, \quad (\text{A8})$$

where p_T was defined with eq. (A3a). The asymptotic behaviors are given by

$$P_\delta(< t) = \frac{2^{11/2}}{3\pi^{3/2}} t^3, \quad \text{for } t \ll 1, \quad (\text{A9a})$$

$$P_\delta(> t) = \frac{2^{11/2}}{45\pi^{3/2}} \frac{1}{t^3}, \quad \text{for } t \gg 1. \quad (\text{A9b})$$

Now let us further adopt a general power law distribution of the lensing masses:

$$p(M) dM \propto M^\alpha dM, \quad \text{for } M_{\min} \leq M \leq M_{\max}. \quad (\text{A10})$$

The normalized mass function can be rewritten in a logarithmic form:

$$p(\log m) d \log m = \left(\frac{\ln 10}{C(\alpha)} \right) m^{\alpha+1} d \log m, \quad m \equiv \frac{M}{M_0}, \quad M_0 \equiv (M_{\min} M_{\max})^{1/2}, \quad (A11)$$

where

$$C(\alpha) = \int_{m_{\min}}^{m_{\max}} m^{\alpha} dm = \begin{cases} \ln(m_{\max}/m_{\min}), & \text{if } \alpha = -1 \\ (m_{\max}^{1+\alpha} - m_{\min}^{1+\alpha})/(1 + \alpha), & \text{otherwise} \end{cases} \quad (A12)$$

After convolving with the mass function, the total number of events is given by:

$$N = \left(\frac{9\pi}{32} \right)^{1/2} n_s \tau \frac{\Delta t}{t_{\sigma,0}} \frac{C(\alpha + 0.5)}{C(\alpha + 1)}, \quad (A13)$$

where τ is the total optical depth by all the lenses with different masses and velocities, and the duration is normalized to

$$t_{\sigma,0} = t_{\sigma}(M = M_0) = \frac{1}{\sigma_V} \left(\frac{GM_0 D_s}{c^2} \right)^{1/2}. \quad (A14)$$

The event duration distribution is given by

$$p(t) = \frac{1}{C(\alpha + 0.5)} \int_{m_{\min}}^{m_{\max}} m^{\alpha} p_{\delta}(m^{-1/2}t) dm, \quad t \equiv \frac{t_0}{t_{\sigma,0}}. \quad (A15)$$

The asymptotic behaviors are given by

$$P(< t) = \frac{2^{11/2}}{3\pi^{3/2}} \frac{C(\alpha - 1)}{C(\alpha + 0.5)} t^3, \quad \text{for } t \ll 1, \quad (A16a)$$

$$P(> t) = \frac{2^{11/2}}{45\pi^{3/2}} \frac{C(\alpha + 2)}{C(\alpha + 0.5)} \frac{1}{t^3}, \quad \text{for } t \gg 1. \quad (A16b)$$

It is convenient to use a logarithmic probability distribution. A few examples of such distribution functions are shown in Figs. 1 and 3.

De Rújula et al (1991) proposed to use the moment analysis to deduce the distribution of lens masses. After some algebra the first two moments can be expressed as

$$\langle \log t \rangle = \langle \log t \rangle_{\delta} + \frac{1}{2} \phi_1, \quad (A17a)$$

$$\langle (\log t)^2 \rangle = \langle (\log t)^2 \rangle_{\delta} + \phi_1 \langle \log t \rangle_{\delta} + \frac{1}{4} \phi_2, \quad (A17b)$$

$$\sigma_{\log t}^2 = \sigma_{\delta}^2 + \frac{1}{4} (\phi_2 - \phi_1^2), \quad \sigma_{\delta} = 0.240, \quad (A17c)$$

where the quantities with a subscript δ were defined with eq. (5), and

$$\phi_1 = \frac{m_{\max}^{1.5+\alpha}(\log m_{\max}) - m_{\min}^{1.5+\alpha}(\log m_{\min})}{m_{\max}^{1.5+\alpha} - m_{\min}^{1.5+\alpha}} - \frac{1}{(1.5 + \alpha) \ln 10}, \quad \alpha \neq -1.5, \quad (A18a)$$

$$\phi_2 = \frac{m_{\max}^{1.5+\alpha}(\log m_{\max})^2 - m_{\min}^{1.5+\alpha}(\log m_{\min})^2}{m_{\max}^{1.5+\alpha} - m_{\min}^{1.5+\alpha}} - \frac{1}{(1.5 + \alpha) \ln 10} \phi_1, \quad \alpha \neq -1.5, \quad (A18b)$$

and

$$\phi_1 = 0.5 \log (m_{\min} m_{\max}), \quad \alpha = -1.5, \quad (A19a)$$

$$\phi_2 = \frac{1}{3} [(\log m_{\min})^2 + (\log m_{\min})(\log m_{\max}) + (\log_{,\max})^2], \quad \alpha = -1.5. \quad (A19b)$$

REFERENCES

- Alcock, C. et al. 1993, *Nature*, 365, 621
- Alcock, C. et al. 1995a, *Phys. Rev. Lett.*, 74, 2867
- Alcock, C. et al. 1995b, *ApJ*, 445, 133
- Alcock, C. et al. 1995c, preprint (= astro-ph/9512146)
- Bennett, D. et al. 1996, talk presented at the 2nd intl. workshop on gravitational microlensing surveys
- Ansari, R. et al. 1995, preprint (= astro-ph/9511073)
- Han, C. & Gould, A. 1995, *ApJ*, 449, 521
- Han, C. & Gould, A. 1996, *ApJ*, submitted (= astro-ph/9504078)
- Kiraga, M. & Paczyński, B. 1994, *ApJ*, 430, 101
- Paczynski, B. 1996, *ARAA*, 34, in press
- Paczynski, B. et al. 1994, *ApJ*, 435, L113
- De Rújula, A., Jetzer, Ph., & Massó, E. 1991, *MNRAS*, 250, 348
- Sahu, K. 1994, *Nature*, 370, 275
- Udalski, A. et al. 1994, *AcA*, 44, 165
- Wu, X.-P. 1994, *ApJ*, 435, 66
- Zhao, H. S., Spergel, D. N., & Rich, R. M. 1995, *ApJ*, 440, L13
- Zhao, H. S., Spergel, D. N., & Rich, R. M. 1996, *MNRAS*, in press

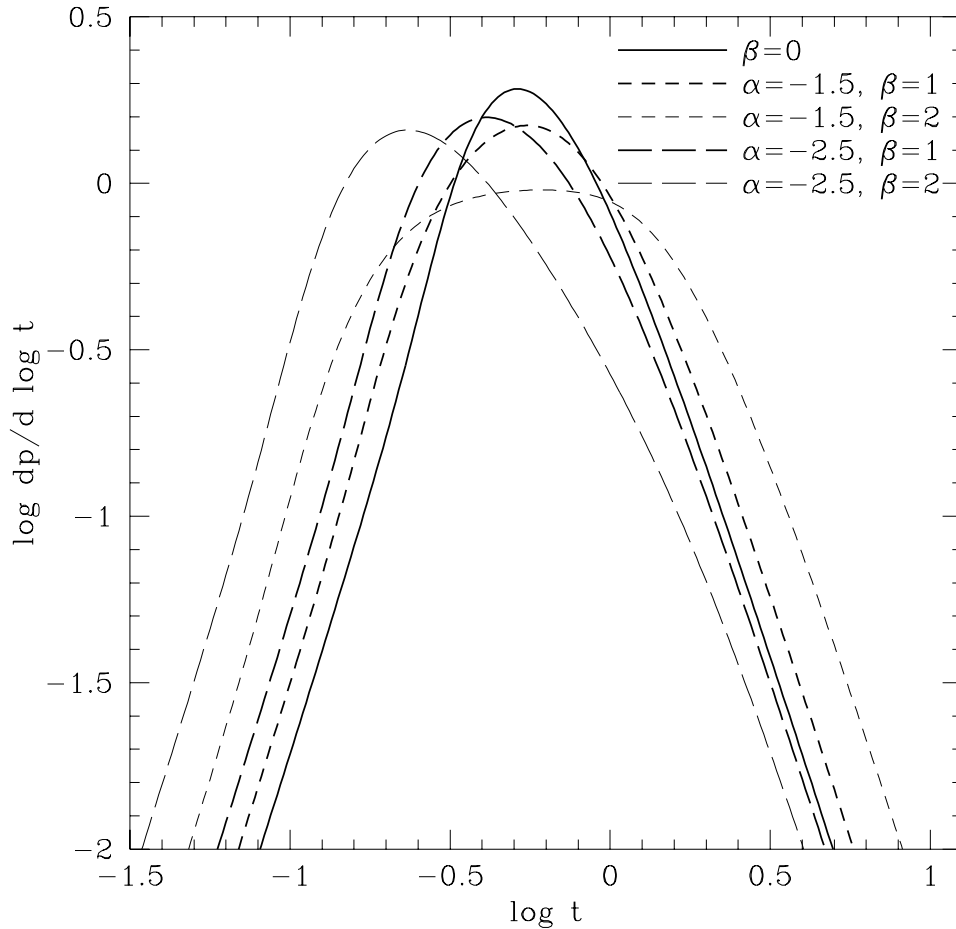


Fig. 1.— The probability distribution functions for the logarithm of event time scale are shown for four power law mass functions: $(\alpha, \beta) = (-1.5, 1)$, $(-1.5, 2)$, $(-2.5, 1)$, $(-2.5, 2)$ where α is the slope of the mass function and $\beta \equiv \log (M_{\max}/M_{\min})$. All the time scales are in units of t_σ corresponding to $M = M_0 \equiv (M_{\min}M_{\max})^{1/2}$ (cf. eqs. 2 and 6). Also shown is the case for $\beta = 0$, which corresponds to all lenses having the same mass (cf. eq. 4).

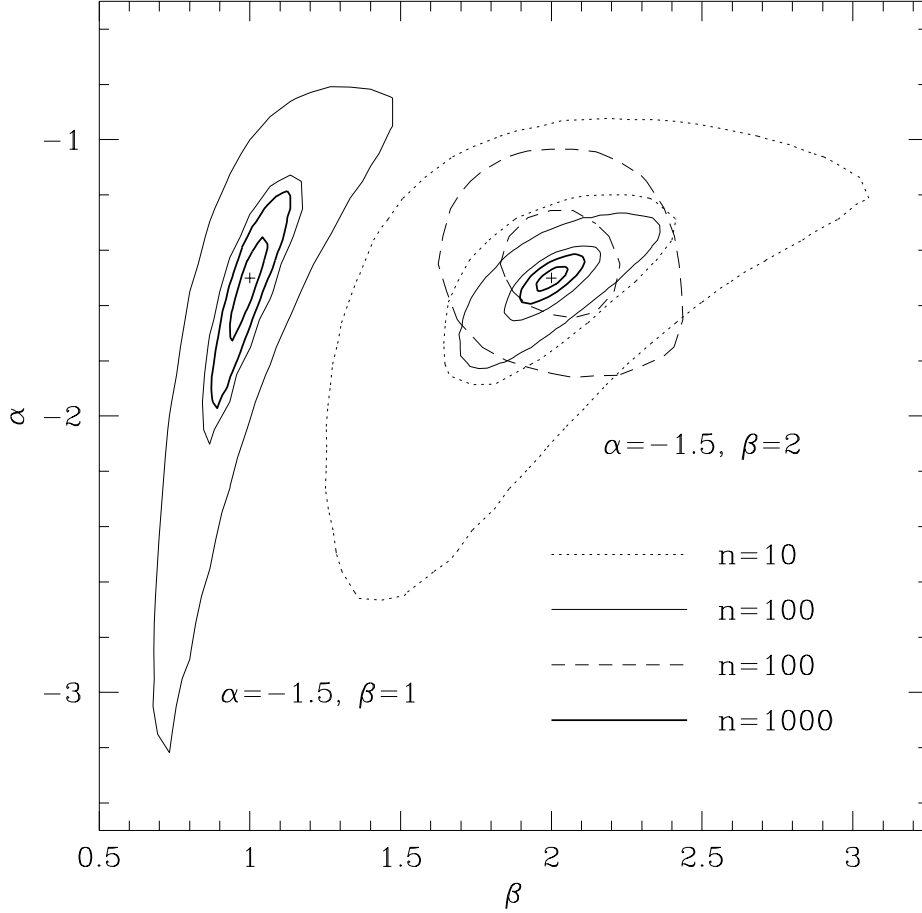


Fig. 2.— The contours corresponding to one and two standard deviations are shown for different models of the mass function in the $\alpha - \beta$ plane, where α is the slope of the mass function and $\beta \equiv \log (M_{\max}/M_{\min})$. The models correspond to $(\alpha, \beta) = (-1.5, 1)$, $(-1.5, 2)$ as indicated by the crosses. The contours are for an average number of microlensing events $n = 10$ (dotted lines), $n = 100$ (thin solid lines), and $n = 1,000$ (thick solid lines). The dotted and solid lines are for models with the mass scale set by fixing the upper mass limit, i.e., declaring it to be known. The dashed contours are for $(\alpha, \beta) = (-1.5, 1)$ with $n = 100$ and with the mass scale set by the first moment (average) of the event durations. In all these simulations we assume that the observers can detect every microlensing event with the impact parameter smaller than its Einstein ring radius, i.e., that the detection system is perfect.

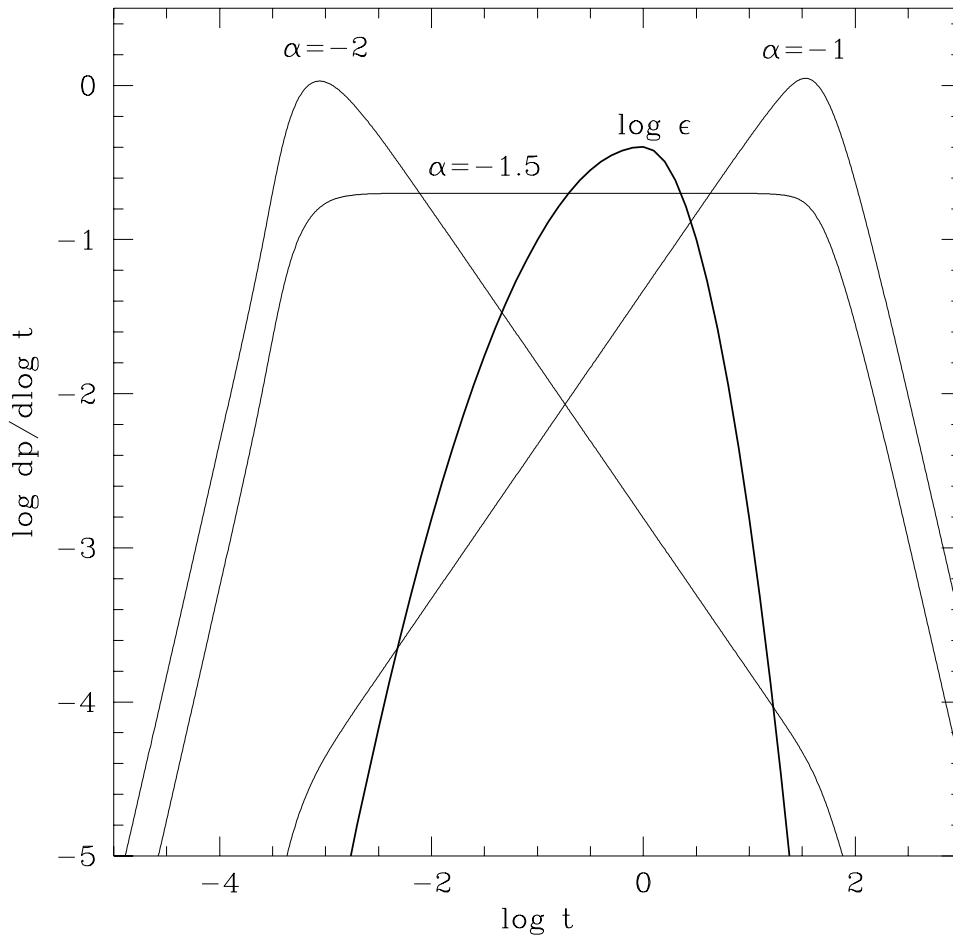


Fig. 3.— The logarithmic probability distributions for event time scales are shown for three very broad mass functions with $\beta = 10$ ($\beta_{\min} = -6, \beta_{\max} = 4$), and the slopes $\alpha = -2, -1.5, -1$, respectively. The time scales are normalized to the duration at the peak sensitivity (cf. eq. 10). Also shown is the approximate shape of the efficiency curve of the MACHO and OGLE searches. Notice, that in this case the majority of lensing events are not detected as they fall outside of the relatively narrow detectability window.

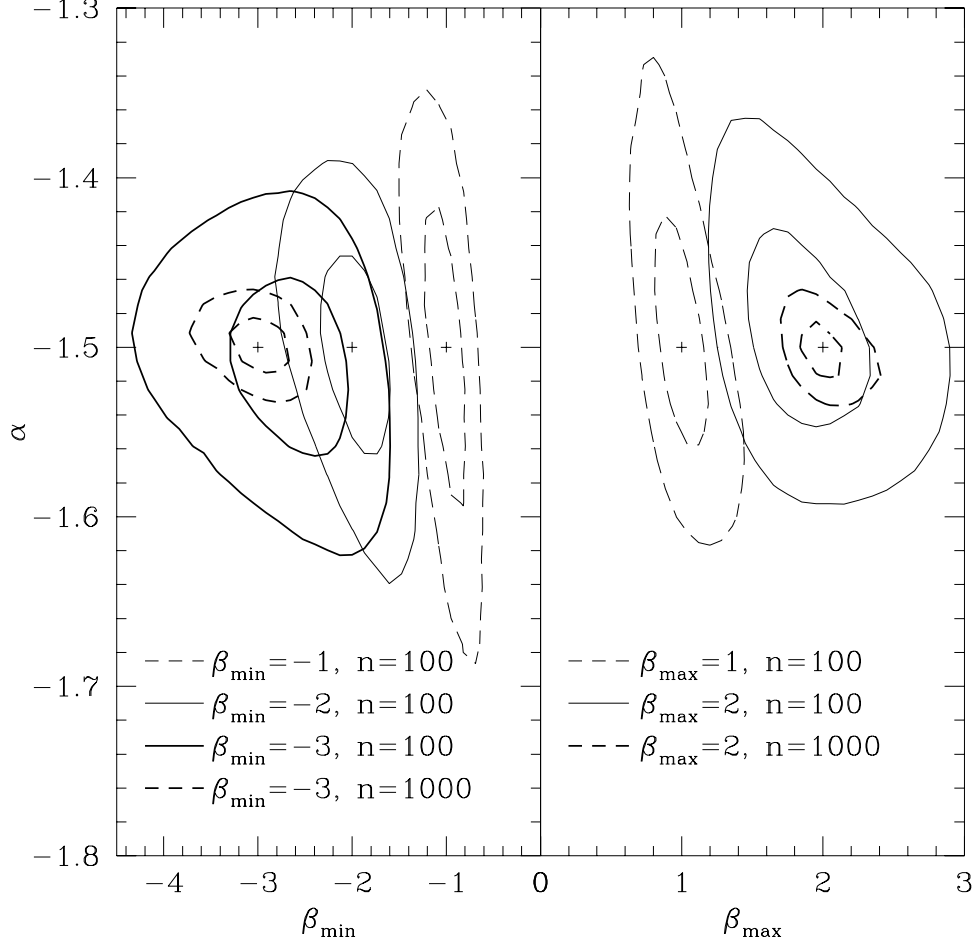


Fig. 4.— The contours corresponding to one and two standard deviations and an average number of microlensing events $n = 100$ and $n = 1000$ are shown in the $\alpha - \beta$ plane, where $\alpha = -1.5$ is the slope of the model lens mass function. For clarity, only two sets of contours for $n = 1000$ are shown. The models on the left correspond to $\beta_{\max} \equiv \log (M_{\max}/M_p) \gg 1$, i.e., the longest events are beyond the detectability window as given with eq. (10) and shown in Fig. 3. The contours are for the mass functions with $\beta_{\min} \equiv \log (M_{\min}/M_p) = -3, -2, -1$. The models on the right correspond to $\beta_{\min} \ll -1$, i.e., the shortest events are beyond the detectability window. The contours are for the mass functions with $\beta_{\max} = 1, 2$.